Carbohydrate Polymers 89 (2012) 24–30

Contents lists available at SciVerse ScienceDirect

Carbohydrate Polymers

journal homepage: www.elsevier.com/locate/carbpol

Interaction between xanthan gum and cationic cellulose JR400 in aqueous solution

Haiping Li[a], Wanguo Hou[a,b,*], Xiuzhi Li[c]

[a] Key Laboratory for Colloid and Interface Chemistry of Education Ministry, Shandong University, Jinan 250100, PR China
[b] Key Laboratory for Eco-chemical Engineering of Education Ministry, Qingdao University of Science and Technology, Qingdao 266042, PR China
[c] Huiqu Junior High School of Anqiu City, Anqiu 262121, Shandong Province, PR China

ARTICLE INFO

Article history:
Received 18 November 2011
Received in revised form
30 December 2011
Accepted 13 February 2012
Available online 23 February 2012

Keywords:
Electrostatic interaction
Hydrogen bond
Xanthan gum
Cationic cellulose
JR400

ABSTRACT

The electrostatic and hydrogen bonding interactions between xanthan gum (XG) and semisynthetic cationic cellulose (JR400) in aqueous solution are investigated via stability map, FT-IR spectra, thermogravimetric analysis, potentiometric measurement and rheological method. The stability map shows three regions, a stable region with XG as the major component, a flocculated region and another stable region with JR400 as the major component. The stability of mixing system depends on both the concentration fraction of JR400 (f_{JR}) and the overlapping concentrations of these two polymers. In the region near the stoichiometric f_{JR}, the mixture shows stoichiometric flocculation, which is independent of the total polymer concentration. However, in the regions away from the stoichiometric f_{JR}, the mixtures are stable when the concentration of major polymer component is higher than its overlapping concentration. In stable regions, the electrostatic and hydrogen bonding interactions can enhance the viscosity of mixing system at appropriate f_{JR} values.

© 2012 Elsevier Ltd. All rights reserved.

1. Introduction

Upon mixing solutions of oppositely charged polyelectrolytes, polyelectrolyte complexes (PECs) can be formed spontaneously (Fuoss & Sadek, 1949; Michaels & Miekka, 1961; Michaels, Mir, & Schneider, 1965) owing to the electrostatic interaction between polyanions and polycations. For some systems, the electrostatic interaction was assisted with hydrogen bonding (Choi, Kano, & Maruyama, 2008), hydrophobic interaction (Liu, Morishima, & Winnik, 2001), iondipole force (Huang, Tan, Zhou, Wang, & Che, 2008), π–π interaction (Moreno-Villoslada et al., 2007) and coupled inclusion complex interaction (Burckbuchler, Boutant, Wintgens, & Amiel, 2006). The formation of PECs is governed by many factors, including the concentration of the polyion solutions, chemical composition, order and rate of mixing, pH, ionic strength, temperature and relative molecular weights of the interacting polyelectrolytes (Michaels et al., 1965).

Since the early work on PECs by Fuoss and Sadek (Fuoss & Sadek, 1949) in 1941 and by Michaels and Miekka (Michaels & Miekka, 1961) in 1961, lots of studies and reviews have been published in this field (Al-Jamal, Ramaswamy, & Florence, 2005; Kötz, Kosmella, & Beitz, 2001; Kabanov & Kabanov, 1998; Kabanov, 2005; Michaels, 1965; Thünemann, Müller, Dautzenberg, Joanny, & Löwen, 2004; Tsuchida & Abe, 1982). Most of the aqueous PEC systems reported so far can be divided into two types on the basis of macroscopic observations: water-soluble PECs and precipitated or phase-separated PECs. In some cases, the phase-separated type is distinct from the complex precipitates and may be further subdivided into stable coacervates, flocculating systems and turbid dispersions upon the state of PECs in aqueous solutions (Doi & Kokufuta, 2010). PECs has been applied in many areas, such as coatings, binders (Doi & Kokufuta, 2010), flocculants (Dinu, Mihai, & Dragan, 2010), delivery and controlled release of drug (El-Hag Ali Said, 2005), multifunctional membranes (Zhao et al., 2010), and capsules (Gericke, Liebert, & Heinze, 2009) protein and gene delivery (Fayazpour et al., 2006; Park, Chun, Cho, & Song, 2010), molecular recognition and isolation (Harada & Kataoka, 1999), porous scaffolds for bone tissue (Coimbra et al., 2011), etc.

PECs are usually prepared in the dilute region of aqueous polyelectrolyte solutions. A change in solution concentration may significantly influence the interactions occurring in solutions. In the semidilute or concentrated region and at the nonstoichiometric ratio of polyanions to polycations, the interaction between polyanions and polycations can lead to the formation of a three-dimensional network (Liu et al., 2001). This is similar to the systems including oppositely charged polyelectrolyte and

* Corresponding author at: Key Laboratory for Colloid and Interface Chemistry of Education Ministry, Shandong University, Jinan 250100, PR China.
Tel.: +86 0531 88365460; fax: +86 0531 88364750.
E-mail address: wghou@sdu.edu.cn (W. Hou).

0144-8617/$ – see front matter © 2012 Elsevier Ltd. All rights reserved.
doi:10.1016/j.carbpol.2012.02.022

surfactant (Antunes, Lindman, & Miguel, 2005; Dreval, Vasil'ev, Litmanovich, & Kulichikhin, 2008; Liu et al., 2001; Liu, Morishima, & Winnik, 2002, 2003; Thuresson, Nilsson, & Lindman, 1996; Tsianou, Kjøniksen, Thuresson, & Nyström, 1999) and those including polyelectrolyte and ionic liquid (Wathier & Grinstaff, 2010). For the semidilute or concentrated polyelectrolyte solutions, the reported systems mainly consist of semisynthetic cationic cellulose and synthetical polyanions with lower molecular weight (Antunes et al., 2005; Dreval et al., 2008; Liu et al., 2001, 2002, 2003; Rodríguez, Alvarez-Lorenzo, & Concheiro, 2001; Thuresson et al., 1996; Tsianou et al., 1999), besides some natural polysaccharides and proteins (Chaisawang & Suphantharika, 2005; Marguerite, 2008; Taylor, Pearson, Draget, Dettmar, & Smidsrød, 2005; Wang, Qiu, Cosgrove, & Denbow, 2009), but related researches are not systematic enough. In this work, the interactions between cationic cellulose JR400 and microbial polysaccharide xanthan gum (XG) in the semidilute and concentrated solution is well investigated. Especially, the mechanism of interaction between them at different composition ratio and concentration is elucidated explicitly.

XG is an anionic extracellular heteropolysaccharide secreted by *Xanthomonas campestris*, consisting of β-1, 4-linked glucopyranose with trisaccharide side chains composed of D-mannose/D-glucuronic acid/D-mannose linked to alternate glucose residues. The D-mannose linked to the main chain contains an acetyl group at position O-6 (see Fig. S1 in supporting information). The degree of acetylation at O-6 of mannose residue and substitution of pyruvate group at the terminal mannose residue depends on fermentation condition (Krstonosic, Dokic, & Milanovic, 2011; Shobha & Tharanathan, 2009). XG solution has high-intrinsic viscosity due to the high molecular weight and the formation of aggregates via hydrogen bonds (Argin-Soysal, Kofinas, & Lo, 2009; Southwick, Lee, Jamieson, & Blackwell, 1980). It shows a pronounced pseudoplastic flow at relatively low concentrations, which makes it suitable as thickener and stabilizer of emulsions or suspensions (Shen, Wan, & Gao, 2010). On mixing XG and other polymers, the hydrogen bonding and electrostatic interactions might occur (Argin-Soysal et al., 2009; Chaisawang & Suphantharika, 2005; Lii, Liaw, Lai, & Tomasik, 2002). JR400 is the chloride salt of a trimethylammonium derivative of hydroxyethylcellulose (see Fig. S1 in supporting information). It functions as cationic, water-soluble and substantive conditioners for hare care and skin care products (Liu et al., 2006).

The goal of this work is to present a new mixing system (XG/JR400 complex), displaying high viscosity at low concentration, which may be used as new thickener, stabilizer, oil-displacing agent, delivery and controlled release system for drugs, and so on. In this mixture, the electrostatic and hydrogen bonding interactions between XG and JR400 were confirmed with the methods of FT-IR, thermoanalysis, potentiometric measurement and rheology. As is expected, the viscosity of XG/JR400 mixture can be enhanced after mixing at appropriate composite ratio and solution concentration.

2. Experimental

2.1. Materials

XG was purchased from Aladdin (China) with the molecular weight ranging from 2×10^6 to 50×10^6 g/mol (Pai, Srinivasarao, & Khan, 2002; Southwick et al., 1980). For each repeating unit, XG has a degree of acetylation of 0.20 and of pyruvation of 0.34 as determined by methods reported in the literature. (McComb & McCready, 1957; Sloneker & Orentas, 1962) JR400 was purchased from Chongqing Haiyue Chemical Industry Co., Ltd. (China) with the molecular weight about 5.0×10^5 g/mol (Dan, Ghosh, & Moulik, 2010; Liu et al., 2001, 2002). The moisture content was determined to be 5.34% by vacuum drying at 105 °C for 24 h. Elemental analysis with an elemental analyzer (VarioEL III, Elementary Analysis System GmbH) showed that the percent contents of carbon, hydrogen and nitrogen are 43.25, 7.97 and 1.10, respectively. Then it can be determined that JR400 has a positive charge content of 19 mol %, corresponding to 19 ammonium groups for every 100 glucose units. Water was purified with a Hitech–Kflow water purification system (China). All other reagents are of analytical grade.

2.2. Solution preparation

The stock solutions (1%) of XG and JR400 were gained by dissolving 4.0 g of XG and JR400 in 396 g of H_2O, respectively. The XG and JR400 solutions at lower concentration were obtained via the dilution of stock solutions. Mixed solutions of XG and JR400 were prepared from weighed aliquots of stock solutions. They were stirred for 12 h after mixing. The stirring speed was adjusted to be as high as possible without forming any bubbles. Finally, the mixed solutions were allowed to stand for 48 h at 25 °C. Their appearance was recorded to construct a stability map. The pH values of the systems were adjusted with 0.1 M HCl and NaOH solutions.

The ratio between the two components is expressed as the weight fraction (f_{JR}) of JR400 in the mixture

$$f_{JR} = \frac{W_{JR}}{W_{XG} + W_{JR}} \quad (1)$$

where W_{XG} and W_{JR} are the weights of XG and JR400 stock solutions, respectively.

2.3. Rheological measurements

The rheological measurements of all the samples were carried out by a RS 75 rheometer (Haake Inc., Germany) equipped with the Z41 concentric cylinder system at 25.0 ± 0.1 °C. Every sample was rested for 20 min before the measurement.

Flow curves were obtained by increasing the shear rate from 0 to 1000 s^{-1} in 300 s. Dynamic measurements were carried out as follows: the stress sweep at the frequency f = 0.5 Hz was conducted from 0 to 10 Pa to determine the linear viscoelastic region. The frequency sweep was performed from 0.01 to 10 Hz at the stress of 0.05 Pa (in the linear viscoelastic region).

2.4. FT-IR spectra

Fresh-dried XG, JR400 and their mixture were tested by Fourier transform infrared (FT-IR) spectrometer (model 20SX, Nicolet) to evaluate the functional groups that might be involved in the interactions.

2.5. TG analysis

The thermal analysis of all the samples was carried out by TGA/SDTA851 thermal analyzer (Mettler Toledo, America). Thermo gravimetric analysis (TGA) was performed up to a temperature of 700 °C, starting from room temperature in an atmosphere of nitrogen. The heating rate was uniform in all cases at 10 °C/min.

2.6. Potentiometric measurements

Potentiometric measurements were performed at 25.0 ± 0.1 °C with pHS-3C pH meter (Leici, China).

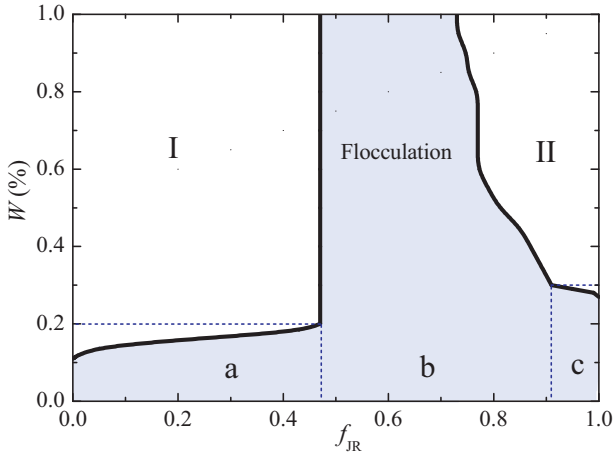

Fig. 1. Stability map for XG/JR400 mixture at different fraction of JR400 (f_{JR}) and total polymer concentrations (W) (pH 6.40 ± 0.10). Width of boundaries: f_{JR} ± 0.01.

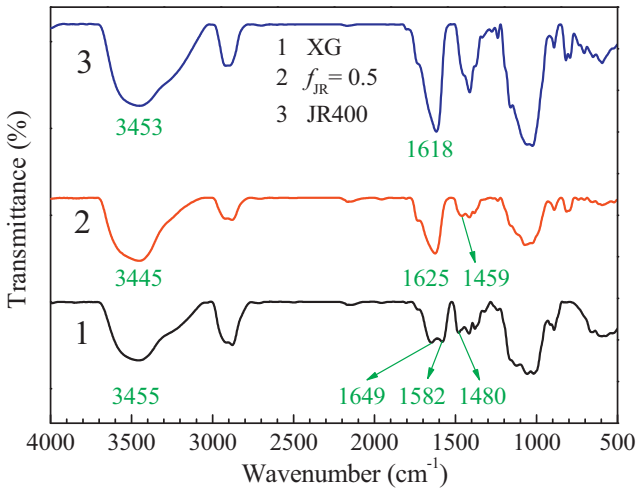

Fig. 2. FT-IR spectra of XG, JR400 and their mixture at f_{JR} = 0.5.

3. Results and discussion

3.1. Stability map of XG/JR400 mixture

Stability map of the XG/JR400 mixture at f_{JR} 0–1 and total polymer concentration (W) less than 1% is shown in Fig. 1. Just like the other mixtures of oppositely charged polyelectrolytes (Liu et al., 2001; Thuresson et al., 1996; Tsianou et al., 1999), three regions, namely, Region I with XG as the major component, Region II with JR400 as the major component and region flocculation, can be found in this stability map. In Regions I and II, the mixture is stable while in region flocculation, flocculation is observed.

The border f_{JR} value between Region I and flocculation is nearly constant and equals to about 0.47 when W is greater than 0.2% (see dash line in Fig. 1), but decreases rapidly with W decreasing when W is less than 0.2%. The border f_{JR} value between Regions II and flocculation increases gradually with W decreasing. In other words, the range of region flocculation increases with W decreasing. According to the contents of carboxyl groups in XG molecules and quaternary ammonium groups in JR400 molecules, the f_{JR} value at the stoichiometric ratio of XG to JR400 is calculated to be about 0.74 if the carboxyl groups were completely ionized. Actually, the carboxyl groups can only be partially ionized, so the stoichiometric f_{JR} value should be less than 0.74. At higher W value, the flocculation only appears near the stoichiometric f_{JR} value; while at lower W value, the flocculation may also appears in the region away from the stoichiometric f_{JR} value. The flocculation near the stoichiometric f_{JR} value may be regarded as stoichiometric flocculation and that in the region away from the stoichiometric f_{JR} value may be regarded as nonstoichiometric flocculation. The subregions of flocculation are roughly identified in Fig. 1, where (a) and (c) represent nonstoichiometric flocculation subregions, and (b) represents stoichiometric flocculation subregion. For this mixture, the flocculation region is narrower than that of mixture including JR400 and poly(2-acrylamido-2-methylpropanesulfonates) at W = 1%. This may be due to the higher molecular weight and hyper-branched structure of XG.

In addition, we find that the border f_{JR} value between Region I and flocculation equals to about C^*_{XG}/W when W is less than 0.2% and that between Regions II and flocculation equals to about C^*_{JR400}/W when W is less than 0.3%. C^*_{XG} (about 0.11%) and C^*_{JR400} (about 0.28%) are the overlapping concentrations of XG solution and JR400 solution, respectively (see Fig. S2 in supporting information). That is to say, in the region away from the stoichiometric f_{JR} value, the mixture is stable at the concentration of major polymer component higher than its overlapping concentration, but nonstoichiometrically flocculated at the former lower than the latter. This may also apply for the reported oppositely charged polyelectrolyte mixtures (Antunes et al., 2005; Dreval et al., 2008; Liu et al., 2001, 2002, 2003; Thuresson et al., 1996; Tsianou et al., 1999). So it can be concluded that the stability map for the mixing system of oppositely charged polyelectrolytes depends to a great degree on both the stoichiometric ratio and overlapping concentrations of these two polymers.

3.2. FT-IR and TG analysis

Fig. 2 shows the FT-IR spectra of XG, JR400 and their mixture at f_{JR} = 0.5. For XG, the peaks at 1649 cm^{-1} and 1582 cm^{-1} are attributed to asymmetric stretching vibration of the pyruvic acid carboxyl and the other carboxyl (see Fig. S1 in supporting information), respectively. The peak at 1480 cm^{-1} is ascribed to the symmetric stretching vibration of carboxyl group. For JR400, the peak at 1618 cm^{-1} is attributed to the C—N stretching vibration. After mixing, the electrostatic interaction between carboxyl groups and quaternary ammonium groups renders the C=O bond weakened just as the hydrogen bonding interaction does (Steiner, 2002), leading to a lowering of the stretching vibration. Then the peak at 1625 cm^{-1} for the mixture is the result of overlapping of the shifted peak from 1616 cm^{-1} for JR400 and the red-shifted peaks from 1582 cm^{-1} and 1649 cm^{-1} for XG. The electrostatic interaction also causes the peak at 1480 cm^{-1} to shift to 1459 cm^{-1}. In addition, the peaks at 3455 cm^{-1} for XG and 3453 cm^{-1} for JR400 correspond to the stretching vibration of hydroxyl groups of polymers. They are all red-shifted to 3445 cm^{-1} after mixing, which indicates that the hydrogen bonds also exist between XG and JR400 besides the electrostatic interaction.

The interaction between XG and JR400 can also be proved by thermogravimetric measurement. Fig. 3 displays the TGA and DTG curves of XG, JR400 and their mixture at f_{JR} = 0.2 and 0.5, respectively. TGA curves of the samples (Fig. 3a) show four decomposition stages: evaporation of trapped water, decarboxylation, dehydration and decomposition of the residues at temperature greater than 460 °C. DTG curves (Fig. 3b) of the samples display the peak temperatures of different stages at which the most fast decomposition rate is reached. The peak temperatures of the main decomposition stage of XG and JR400 are 343 °C and 282 °C, respectively. For the

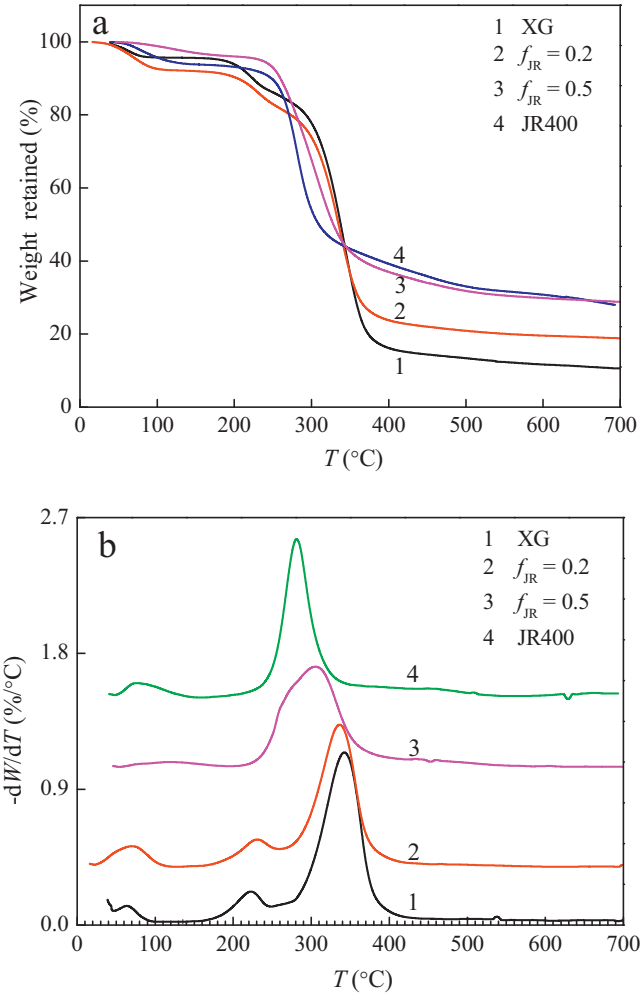

Fig. 3. TGA (a) and DTG (b) curves of XG, JR400 and their mixture at f_{JR} = 0.2 and 0.5.

mixtures, only one peak temperature of main decomposition stage for each sample is observed, namely, 336 °C for f_{JR} = 0.2 and 305 °C for f_{JR} = 0.5, which indicates that the complex between XG and JR400 is formed (Habi & Djadoun, 2008; Xiao, Lu, & Zhang, 2001).

3.3. Potentiometric measurement

Potentiometry has been widely used for the study of interpolymer complexes formed via hydrogen bonding or electrostatic interactions (Chen, Liu, Jin, & Chen, 2007). Fig. 4 shows the variation of pH of the XG/JR400 mixture (W = 0.1%) with f_{JR} at different pH levels. It can be seen that at pH less than 6.8, pH of mixture is decreased after mixing while at pH greater than 7.5, pH of mixture is increased.

According to the complexation equilibrium between polyacids and polybases (Vasile, Bumbu, Mylonas, Cojocaru, & Staikos, 2003) and the main interactions between XG and JR400, the main complexation equilibrium among XG/JR400 mixture can be denoted as follows:

$$-\mathrm{COOH} \rightleftharpoons H^+ + -\mathrm{COO}^- \quad (4)$$

$$\mathrm{XG\text{-}COO^-} + \mathrm{JR400\text{-}N^+} \rightleftharpoons \mathrm{XG\text{-}COO^-\cdots{}^+N\text{-}JR400} \quad (5)$$

$$\mathrm{XG\text{-}COO^-} + \mathrm{JR400\text{-}OH} \rightleftharpoons \mathrm{XG\text{-}COO\cdots HO\text{-}JR400} \quad (6)$$

$$\mathrm{XG\text{-}COOH} + \mathrm{JR400\text{-}OR} \rightleftharpoons \mathrm{XG\text{-}COOH\cdots \underset{A}{O}\text{-}JR400} \quad (7)$$

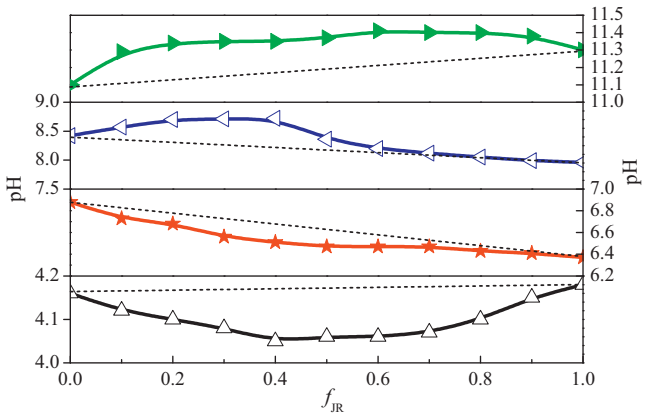

Fig. 4. Dependence of pH on f_{JR} for XG/JR400 mixture at different pH levels and total concentration of 0.1%.

Equilibrium (4) is the weak polyacids dissociation equilibrium; Equilibrium (5) represents the electrostatic interaction between XG and JR400; Equilibriums (6) and (7) reveal the hydrogen bonds between XG and JR400. Alkyl or "H" is noted as "A" in JR400-OA. At pH less than 6.8, the carboxyl groups of XG adopt mainly as —COOH, i.e. the concentration of —COO^- is very low. After mixing of XG and JR400, the formation of Equilibrium (7) can only decrease the concentration of —COOH slightly in comparison with its high original concentration while Equilibriums (5) and (6) will decrease the concentration of —COO^- obviously due to its low concentration. This causes Equilibrium (4) to move right, so pH of the system gets decreased after mixing XG and JR400. By contrast, at pH greater than 7.5, the carboxyl groups of XG adopt mainly as —COO^-. Thus, pH of the system depends on Equilibrium (7) chiefly. Equilibrium (7) causes Equilibrium (4) to move left, so pH of the system increases after mixing of XG and JR400. These potentiometric results indicate that there is not only electrostatic interaction between XG and JR400, but also the hydrogen bonding interaction which is consistent with FT-IR analysis (Fig. 2).

3.4. Rheological measurement

In order to identify the rheological behavior of the fluids in Region I and Region II, the rheological measurements were carried out. Fig. 5 shows the flow curves of XG/JR400 mixture at W of 1% in the f_{JR} ranges of 0–0.4 and 0.78–1, respectively. These curves are fitted by Herschel–Bulkley model and Ostwald–de-Waele model as follows, Herschel–Bulkley model

$$\tau = \tau_0 + k\dot{\gamma}^n \quad (2)$$

Ostwald–de-Waele model

$$\tau = K\dot{\gamma}^N \quad (3)$$

where τ is the shear stress, τ_0 the yield stress, k and K the consistency coefficients, n and N the flow index, and $\dot{\gamma}$ the shear rate. For the samples in Region I (Fig. 5a), the fitting results of Eqs. (2) and (3) are listed in Table 1. It can be concluded from the Adj. R^2 values that the flow curves at f_{JR} 0–0.4 can be fitted better by Herschel–Bulkley model. The values of τ_0 is in the range of 7.35–1.39 Pa. The higher τ_0 values demonstrate the fluids display gel-like behavior in Region I. For the samples in Region II (Fig. 5b), the fitting results of Eq. (3) are listed in Table 1. Because of all the Adj. R^2 values greater than 0.999 at f_{JR} 0.78–1, it is thought that the curves can be fitted very well by Ostwald–de-Waele model, i.e., no yield stress exists for fluids in Region II. Therefore, the fluids in Region II are viscous but not

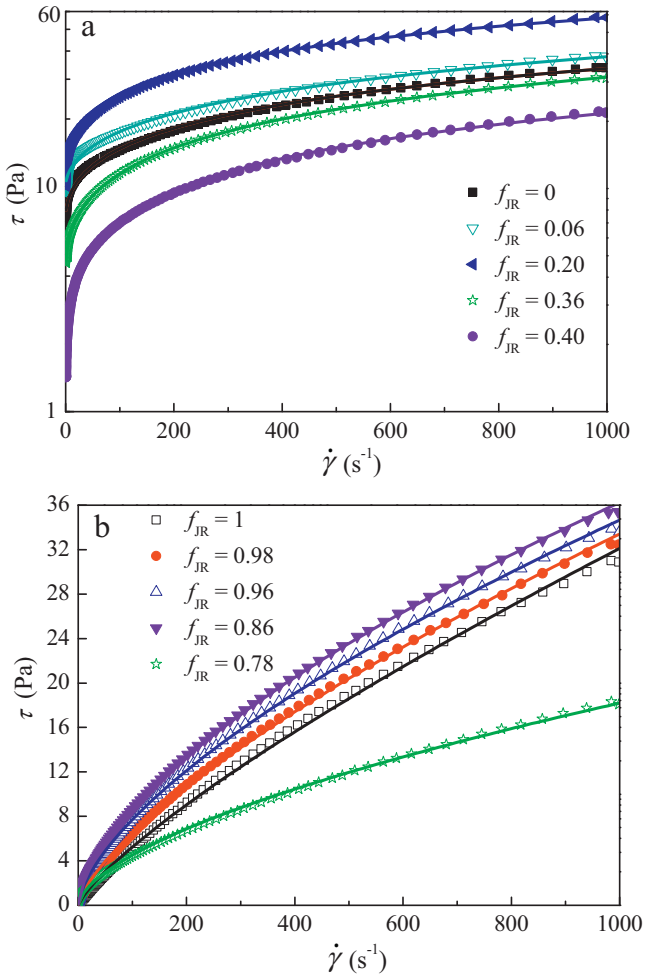

Fig. 5. Flow curves of XG/JR400 mixture at total polymer concentration of 1% and different f_{JR}.

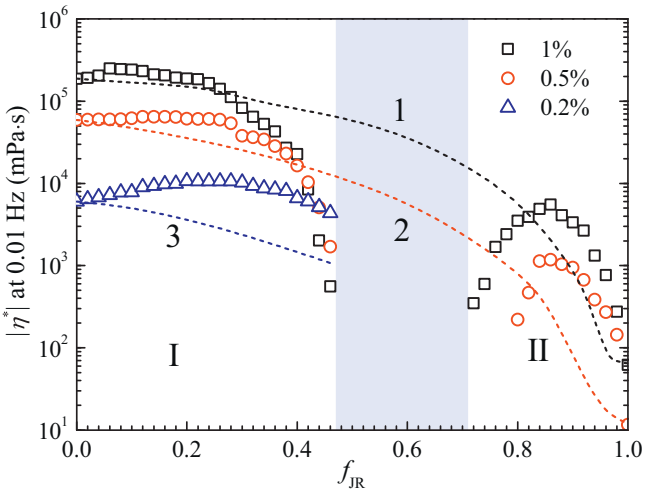

Fig. 6. Dependence of dynamic viscosity of XG/JR400 mixture on f_{JR} at shear stress of 0.05 Pa and different total concentrations (pH 6.40 ± 0.10). Dash lines show the ideal dynamic viscosity of the mixture.

gel-like. The molecular weight of XG is much higher than that of JR400. This may be the reason of formation of gel-like fluid in Region I and viscous fluid in Region II.

In addition, as f_{JR} increases in Region I or decreases in Region II, the τ_0 and consistency coefficients of the fluids increase initially and decrease subsequently, which shows that the microstructural strength increases initially and decreases subsequently.

Table 1
Fitting results of flow curves for XG/JR400 mixture at f_{JR} less than 0.5 or greater than 0.7.

Model	f_{JR}	τ_0	k, K	n, N	Adj. R^2
Herschel–Bulkley	0	7.35	0.591	0.548	0.996
	0.06	9.10	1.93	0.463	0.999
	0.20	10.1	0.543	0.569	0.996
	0.36	4.28	0.528	0.566	0.999
	0.40	1.39	0.432	0.554	0.999
Ostwald–de-Waele	0	0	5.59	0.238	0.933
	0.06	0	7.62	0.209	0.917
	0.20	0	7.81	0.274	0.973
	0.36	0	2.86	0.327	0.959
	0.40	0	1.02	0.432	0.978
	1	0	0.139	0.787	0.999
	0.98	0	0.245	0.711	0.999
	0.96	0	0.381	0.653	0.999
	0.86	0	0.497	0.621	0.999
	0.78	0	0.277	0.606	0.999

Fig. 6 shows the variations of dynamic viscosity ($|\eta^*|$) of XG/JR400 mixture with f_{JR} and W at the shear stress of 0.05 Pa, the frequency of 0.01 Hz and pH 6.40 ± 0.10. As can be seen, the dynamic viscosity of the mixtures increases initially and decreases subsequently as f_{JR} increases in Region I or decreases in Region II. With W increasing, the dynamic viscosity of the mixtures increases. In addition, the ideal dynamic viscosity of the mixtures is also shown in Fig. 6. The idea dynamic viscosity here is the sum of dynamic viscosity of pure XG solution at the concentration of $W(1-f_{JR})$ and that of pure JR400 solution at the concentration of Wf_{JR}. The ideal dynamic viscosity represents the dynamic viscosity of the mixtures without any interaction between XG and JR400. Any deviation of the actual dynamic viscosity of mixtures from their ideal value arises from the interactions between the two polymers. It can be seen from Fig. 6 that both in Region I and region II, the mixtures at appropriate f_{JR} values may show a higher actual dynamic viscosity than the idea dynamic viscosity, which indicates that the mixing of XG and JR400 can enhance the microstructural strength of the system.

In Region I and II, the concentrations of major polymer components, i.e., XG in Region I and JR400 in Region II, are above their overlapping concentrations, so the major polymer chains are entangled to form three-dimensional networks (Scheme 1). A small amount of oppositely charged polymer added in the system can interact with the major polymer via electrostatic forces and hydrogen bonds, just as a cross-linker, to reinforce the structural strength of the three dimensional networks (Scheme 1). So the dynamic viscosity, τ_0 (Table 1), and consistency coefficient (Table 1) of the mixtures increases initially as f_{JR} increases in Region I or decreases in Region II. It is the cross-linking of the oppositely charged polymer to the major polymer that results in the higher actual dynamic viscosity than the idea one. The subsequent decrease of dynamic viscosity, τ_0 (Table 1), and consistency coefficient (Table 1) of the mixtures with f_{JR} further increasing in Region I or further decreasing in Region II can be attributed to the formation of aggregates via electrostatic forces between XG and JR400, which can partially destruct the three-dimensional (3D) networks of the system. It is the strong aggregation of excess oppositely charged polymer with the major polymer that induces the actual dynamic viscosity lower than the ideal one (see Fig. 6).

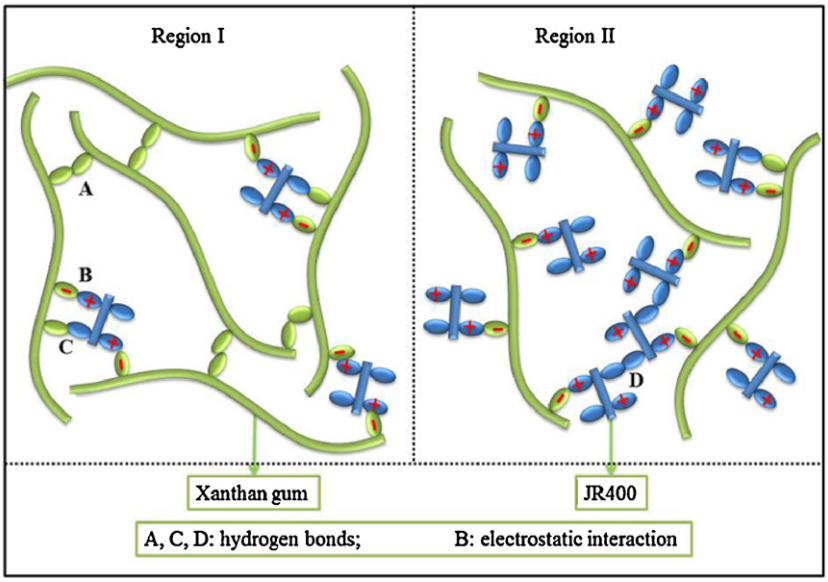

Scheme 1. Microstructures of stable fluids in Regions I and II.

4. Conclusions

The electrostatic and hydrogen bonding interactions between XG and JR400 in aqueous solution are confirmed via stability map, FT-IR spectra, thermogravimetric analysis, potentiometric measurement and rheological method. Three regions are observed in the stability map, namely, a stable region with XG as the major component, a flocculated region and another stable region with JR400 as the major component. It is found that the stability of the mixing system consisting of oppositely charged polyelectrolytes depends on both the f_{JR} value and overlapping concentrations of these two polymers. In the region near the stoichiometric f_{JR} value, the mixture shows stoichiometric flocculation, which is independent of the *W* value. However, in the regions away from the stoichiometric f_{JR} value, the mixtures are stable at the concentration of major component higher than its overlapping concentration. In stable regions, the interactions between the oppositely charged polyelectrolytes can enhance the structural strength of the system at appropriate f_{JR} values.

Acknowledgements

This work was supported by the National Natural Science Foundation of China (No. 21173135), the Natural Science Foundation of Shandong Province of China (No. ZR2009BZ001) and Taishan Scholar Foundation of Shandong Province of China (No. ts20070713).

Appendix A. Supplementary data

Supplementary data associated with this article can be found, in the online version, at doi:10.1016/j.carbpol.2012.02.022.

References

Al-Jamal, K. T., Ramaswamy, C., & Florence, A. T. (2005). Supramolecular structures from dendrons and dendrimers. *Advanced Drug Delivery Reviews*, *57*, 2238–2270.
Antunes, F. E., Lindman, B., & Miguel, M. G. (2005). Mixed systems of hydrophobically modified polyelectrolytes: controlling rheology by charge and hydrophobe stoichiometry and interaction strength. *Langmuir*, *21*, 10188–10196.
Argin-Soysal, S., Kofinas, P., & Lo, Y. M. (2009). Effect of complexation conditions on xanthan-chitosan polyelectrolyte complex gels. *Food Hydrocolloids*, *23*, 202–209.
Burckbuchler, V., Boutant, V., Wintgens, V., & Amiel, C. (2006). Macromolecular assemblies based on coupled inclusion complex and electrostatic interactions. *Biomacromolecules*, *7*, 2890–2900.
Chaisawang, M., & Suphantharika, M. (2005). Effects of guar gum and xanthan gum additions on physical and rheological properties of cationic tapioca starch. *Carbohydrate Polymers*, *61*, 288–295.
Chen, S., Liu, M., Jin, S., & Chen, Y. (2007). Structure and properties of the polyelectrolyte complex of chitosan with poly(methacrylic acid). *Polymer International*, *56*, 1305–1312.
Choi, S. W., Kano, A., & Maruyama, A. (2008). Activation of DNA strand exchange by cationic comb-type copolymers:effect of cationic moieties of the copolymers. *Nucleic Acids Research*, *36*, 342–351.
Coimbra, P., Ferreira, P., de Sousa, H. C., Batista, P., Rodrigues, M. A., Correia, I. J., et al. (2011). Preparation and chemical and biological characterization of a pectin/chitosan polyelectrolyte complex scaffold for possible bone tissue engineering applications. *International Journal of Biological Macromolecules*, *48*, 112–118.
Dan, A., Ghosh, S., & Moulik, S. P. (2010). Interaction of cationic hydroxyethylcellulose (JR400) and cationic hydrophobically modified hydroxyethylcellulose (LM200) with the amino-acid based anionic amphiphile sodium N-dodecanoyl sarcosinate (SDDS) in aqueous medium. *Carbohydrate Polymers*, *80*, 44–52.
Dinu, I. A., Mihai, M., & Dragan, E. S. (2010). Comparative study on the formation and flocculation properties of polyelectrolyte complex dispersions based on synthetic and natural polycations. *Chemical Engineering Journal*, *160*, 115–121.
Doi, R., & Kokufuta, E. (2010). On the water dispersibility of a 1:1 stoichiometric complex between a cationic nanogel and linear polyanion. *Langmuir*, *26*, 13579–13589.
Dreval, V., Vasil'ev, G., Litmanovich, E., & Kulichikhin, V. (2008). Rheological properties of concentrated aqueous solutions of anionic and cationic polyelectrolyte mixtures. *Polymer Science Series A*, *50*, 751–756.
El-Hag Ali Said, A. (2005). Radiation synthesis of interpolymer polyelectrolyte complex and its application as a carrier for colon-specific drug delivery system. *Biomaterials*, *26*, 2733–2739.
Fayazpour, F., Lucas, B., Alvarez-Lorenzo, C., Sanders, N. N., Demeester, J., & De Smedt, S. C. (2006). Physicochemical and transfection properties of cationic hydroxyethylcellulose/DNA nanoparticles. *Biomacromolecules*, *7*, 2856–2862.
Fuoss, R. M., & Sadek, H. (1949). Mutual interaction of polyelectrolytes. *Science*, *110*, 552–554.
Gericke, M., Liebert, T., & Heinze, T. (2009). Polyelectrolyte synthesis and in situ complex formation in Ionic liquids. *Journal of the American Chemical Society*, *131*, 13220–13221.
Habi, A., & Djadoun, S. (2008). Miscibility and thermal behaviour of poly(styrene-co-methacrylic acid)/poly(isobutyl methacrylate-co-4-vinylpyridine) mixtures. *Thermochimica Acta*, *469*, 1–7.
Harada, A., & Kataoka, K. (1999). Chain length recognition: core-shell supramolecular assembly from oppositely charged block copolymers. *Science*, *283*, 65–67.
Huang, X., Tan, Y., Zhou, Q., Wang, Y., & Che, Y. (2008). Aggregation behavior of sodium alginate with cucurbituril in aqueous solution. *Carbohydrate Polymers*, *74*, 685–690.
Kötz, J., Kosmella, S., & Beitz, T. (2001). Self-assembled polyelectrolyte systems. *Progress in Polymer Science*, *26*, 1199–1232.
Kabanov, A. V., & Kabanov, V. A. (1998). Interpolyelectrolyte and block ionomer complexes for gene delivery: physico-chemical aspects. *Advanced Drug Delivery Reviews*, *30*, 49–60.
Kabanov, V. A. (2005). Polyelectrolyte complexes in solution and in bulk. *Russian Chemical Reviews*, *74*, 3–20.

Krstonosic, V., Dokic, L., & Milanovic, J. (2011). Micellar properties of OSA starch and interaction with xanthan gum in aqueous solution. *Food Hydrocolloids*, *25*, 361–367.

Lii, C. Y., Liaw, S. C., Lai, V. M. F., & Tomasik, P. (2002). Xanthan gum-gelatin complexes. *European Polymer Journal*, *38*, 1377–1381.

Liu, R. C. W., Morishima, Y., & Winnik, F. M. (2001). A rheological evaluation of the interactions in water between a cationic cellulose ether and sodium poly(2-acrylamido-2-methylpropanesulfonates). *Macromolecules*, *34*, 9117–9124.

Liu, R. C. W., Morishima, Y., & Winnik, F. M. (2002). Rheological properties of mixtures of oppositely charged polyelectrolytes A study of the interactions between a cationic cellulose ether and a hydrophobically modified poly[sodium 2-(acrylamido)-2-methylpropanesulfonate]. *Polymer Journal*, *34*, 340–346.

Liu, R. C. W., Morishima, Y., & Winnik, F. M. (2003). Composition-dependent rheology of aqueous systems of amphiphilic sodium poly(2-acrylamido-2-methylpropanesulfonates) in the presence of a hydrophobically modified cationic cellulose ether. *Macromolecules*, *36*, 4967–4975.

Liu, X. M., Gao, W., Maziarz, E. P., Salamone, J. C., Duex, J., & Xia, E. (2006). Detailed characterization of cationic hydroxyethylcellulose derivatives using aqueous size-exclusion chromatography with on-line triple detection. *Journal Of Chromatography A*, *1104*, 145–153.

Marguerite, R. (2008). Rheological investigation on hyaluronan-fibrinogen interaction. *International Journal of Biological Macromolecules*, *43*, 444–450.

McComb, E. A., & McCready, R. M. (1957). Determination of acetyl in pectin and in acetylated carbohydrate polymers. *Analytical Chemistry*, *29*, 819–821.

Michaels, A. S. (1965). Polyelectrolyte complexes. *Industrial & Engineering Chemistry*, *57*, 32–40.

Michaels, A. S., & Miekka, R. G. (1961). Polycation-polyanion complexes: preparation and properties of poly-(vinylbenzyltrimethylammonium)/poly-(styrenesulfonate). *The Journal of Physical Chemistry*, *65*, 1765–1773.

Michaels, A. S., Mir, L., & Schneider, N. S. (1965). A conductometric study of polycation-polyanion reactions in dilute aqueous solution. *The Journal of Physical Chemistry*, *69*, 1447–1455.

Moreno-Villoslada, I., González, F., Rivera, L., Hess, S., Rivas, B. L., Shibue, T., et al. (2007). Aromatic–aromatic interaction between 2, 3, 5-triphenyl-2H-tetrazolium chloride and poly(sodium 4-styrenesulfonate). *The Journal of Physical Chemistry B*, *111*, 6146–6150.

Pai, V., Srinivasarao, M., & Khan, S. A. (2002). Evolution of microstructure and rheology in mixed polysaccharide systems. *Macromolecules*, *35*, 1699–1707.

Park, M. R., Chun, C. J., Cho, C. S., & Song, S. C. (2010). Enhancement of sustained and controlled protein release using polyelectrolyte complex-loaded injectable and thermosensitive hydrogel. *European Journal of Pharmaceutics and Biopharmaceutics*, *76*, 179–188.

Rodríguez, R., Alvarez-Lorenzo, C., & Concheiro, A. (2001). Rheological evaluation of the interactions between cationic celluloses and carbopol 974P in water. *Biomacromolecules*, *2*, 886–893.

Shen, D., Wan, C., & Gao, S. (2010). Molecular weight effects on gelation and rheological properties of konjac glucomannan-xanthan mixtures. *Journal of Polymer Science Part B: Polymer Physics*, *48*, 313–321.

Shobha, M. S., & Tharanathan, R. N. (2009). Rheological behaviour of pullulanase-treated guar galactomannan on co-gelation with xanthan. *Food Hydrocolloids*, *23*, 749–754.

Sloneker, J. H., & Orentas, D. G. (1962). Pyruvic acid, a unique component of an exocellular bacterial polysaccharide. [10.1038/194478a0]. *Nature*, *194*, 478–479.

Southwick, J. G., Lee, H., Jamieson, A. M., & Blackwell, J. (1980). Self-association of xanthan in aqueous solvent-systems. *Carbohydrate Research*, *84*, 287–295.

Steiner, T. (2002). The hydrogen bond in the solid state. *Angewandte Chemie international Edition*, *41*, 48–76.

Taylor, C., Pearson, J. P., Draget, K. I., Dettmar, P. W., & Smidsrød, O. (2005). Rheological characterisation of mixed gels of mucin and alginate. *Carbohydrate Polymers*, *59*, 189–195.

Thünemann, A. F., Müller, M., Dautzenberg, H., Joanny, J. F., & Löwen, H. (2004). Polyelectrolyte complexes. In M. Schmidt (Ed.), *Polyelectrolytes with defined molecular architecture II* (pp. 19–33). Berlin/Heidelberg: Springer.

Thuresson, K., Nilsson, S., & Lindman, B. (1996). Effect of hydrophobic modification on phase behavior and rheology in mixtures of oppositely charged polyelectrolytes. *Langmuir*, *12*, 530–537.

Tsianou, M., Kjøniksen, A. L., Thuresson, K., & Nyström, B. (1999). Light ccattering and viscoelasticity in aqueous mixtures of oppositely charged and hydrophobically modified polyelectrolytes. *Macromolecules*, *32*, 2974–2982.

Tsuchida, E., & Abe, K. (1982). Interactions between macromolecules in solution and intermacromolecular complexes. In E. Tsuchida, & K. Abe (Eds.), *Interactions between macromolecules in solution and intermacromolecular complexes* (pp. 1–119). Berlin/Heidelberg: Springer.

Vasile, C., Bumbu, G. G., Mylonas, Y., Cojocaru, I., & Staikos, G. (2003). Hydrogen-bonding interaction of an alternating maleic acid-vinyl acetate copolymer with poly(ethylene glycol), polyacrylamide and poly(N-isopropylacrylamide): a comparative study. *Polymer International*, *52*, 1887–1891.

Wang, Y., Qiu, D., Cosgrove, T., & Denbow, M. L. (2009). A small-angle neutron scattering and rheology study of the composite of chitosan and gelatin. *Colloids and Surfaces B: Biointerfaces*, *70*, 254–258.

Wathier, M., & Grinstaff, M. W. (2010). Synthesis and creep-recovery behavior of a neat viscoelastic polymeric network formed through electrostatic interactions. *Macromolecules*, *43*, 9529–9533.

Xiao, C., Lu, Y., & Zhang, L. (2001). Preparation and physical properties of konjac glucomannan-polyacrylamide blend films. *Journal of Applied Polymer Science*, *81*, 882–888.

Zhao, Q., An, Q., Sun, Z., Qian, J., Lee, K. R., Gao, C., et al. (2010). Studies on structures and ultrahigh permeability of novel polyelectrolyte complex membranes. *The Journal of Physical Chemistry B*, *114*, 8100–8106.